Comparisons of the proton-induced dark current and charge transfer efficiency responses of n- and p-channel CCDs

Cheryl J. Marshall[*a], Paul W. Marshall[b], Augustyn Waczynski[c], Elizabeth Polidan[c], Scott Johnson[c], and Art Campbell[d]
[a]NASA Goddard Space Flight Center, Code 561, Greenbelt, MD, USA 20771
[b]Consultant, Brookneal, VA 24528
[c]Global Science and Technology, NASA Goddard Space Flight Center, Greenbelt, MD 20770
[d]Naval Research Laboratory, Washington, DC

ABSTRACT

The proton-induced charge transfer efficiency (CTE) behavior for the Lawrence Berkeley National Laboratory (LBNL) p-channel CCD (being developed for the SuperNova Acceleration Probe (SNAP)) is compared with the Hubble Space Telescope's (HST) Wide Field Camera 3 (WFC3) n-channel CCDs CTE using ^{55}Fe x-rays, first pixel edge response (FPR), and extended pixel edge response (EPER) techniques. The pre- and post-proton radiation performance parameters of p-channel CCDs designed by LBNL and fabricated at Dalsa Semiconductor, Inc.are compared with n-channel CCDs from E2V, Inc. LBNL p-channel CCDs both with and without notched parallel registers are compared with the E2V CCD43 (a notched, multi-phase pinned (MPP) device) and the E2V CCD44 (an un-notched, non-MPP device), using the same readout timing and measured over the same range of temperatures. The CTE performance of the p-channel CCD is about an order of magnitude better than similar n-channel CCDs for the conditions measured here after a 63 MeV proton fluence of 2.5 x 10^9 cm^{-2}, which is equivalent to 2.5 years in the HST orbit behind shielding comparable to about 2.5 cm Al. Our measurements are compared with previous CTE measurements at 12 MeV by Bebek et al. [1]. The ~ 10 x CTE improvements relative to n-channel CCDs is seen at -83°C, a temperature which is optimized for n-channel CCD performance. Advantages from p-channel CCDs should be greater at other temperatures. Dark current measurements and hot pixel issues are also discussed.

Keywords: p-channel CCDs, p-channel CCDs, focal plane arrays, radiation effects, CCD, proton displacement damage

1. INTRODUCTION

The great successes in conventional n-channel CCD technology (quantum efficiency close to unity in the visible, negligible dark current, charge transfer efficiency (CTE) >0.999999, full well >10^6 electrons, read noise from 2 – 5 electrons RMS) are remarkable. Unfortunately, it is often the case that the greater the performance (and science capability), the greater the sensitivity to radiation. Radiation-induced detector degradation limits the type, precision and/or lifetime of science data collection. One of the key parameters that degrades in a proton environment is the CTE which is limited for most applications by the capture and re-emission of signal charge by the radiation-induced phosphorous-vacancy complex known also as the E center. In 1997, Spratt et al. proposed the use of p-channel CCDs for improved radiation response to both total ionizing dose and displacement damage effects [2]. In particular, it was proposed that the dominant defect to compromise the CTE would be the second order (and therefore less favorably formed) divacancy. In addition, its energy level and capture cross section, would not be as effective at lowering the CTE in a p-channel CCD as the E center is in the n-channel CCD in the temperature range generally of interest. However, as noted by Bebek et al. [1,3], other hole traps are possible, such as the interstitial carbon, that may adversely affect the CTE in a p-channel CCD.

* Cmarshall2@aol.com; phone 1 434 376-3402

The first experimental evidence for the superiority of the CTE response of the p-channel CCD was presented by Hopkinson [4] who showed that the proton-induced degradation of an E2V p-channel CCD was at least a factor of three less than that for a conventional n-channel CCD. That CCD was fabricated on n/n+ silicon using primarily the standard E2V n-channel process except for the boron buried channel and source/drain implants. More recently, Bebek et al. [3] of the Lawrence Berkeley National Laboratory (LBNL) have observed significant improvement in the CTE degradation as compared to n-channel CCDs. (Quantitative comparisons with n-channel CCD data in the literature were hampered by the fact that the available n-channel CCD data was for very low amounts of displacement damage dose compared to their p-channel CCD exposures. Also, readout times and temperatures differed for the various measurements.) The p-channel CCD data of Bebek et al. [1] were measured at 128 K using the ^{55}Fe x-ray technique with an x-ray density of about 1 event per 70 pixels. In addition, the LBNL group found a factor of two improvement in CTE loss for devices with a notch built in the parallel registers. In contrast to the device studied by Hopkinson [4], the p-channel CCD developed by Bebek et al. [1, and references therein] is on high resistivity starting material resulting in a depletion depth of about 300 μm so that it is optimized for red and near-IR detection.

In this paper, we have undertaken an independent assessment of the proton response of the p-channel CCD developed by LBNL using high resistivity n-Si with boron implants to create a p-channel CCD. Both the proton-induced CTE degradation and dark current distributions have been studied. The CTE measurements were made using the extended pixel edge response (EPER) and first pixel response (FPR) methods in addition to the ^{55}Fe x-ray technique. The CTE measurements were taken using the same readout timing as previous n-channel CCD work [5,6] on the Hubble Space Telescope Wide Field Camera 3 imager (WFC3 timing) as well as the timing employed by LBNL in their p-channel CCD work [1,3] so that direct comparisons can be made. Reproducing the readout timing and measurement temperatures, as well as the ^{55}Fe x-ray density, are important considerations due to the time and temperature dependencies of the trap capture and emission processes. Dark current histograms were acquired as a function of temperature and compared to those obtained for the WFC3 n-channel CCDs.

2. EXPERIMENT DESCRIPTION

The LBNL p-channel CCDs devices in this study are 512 x 1024 pixel arrays with a 15 μm pixel pitch. All the devices have a notch in the serial register but devices with and without a notch in the parallel registers were tested. The notches are formed by an additional boron implant that serves to confine the charge in small signals to a narrow region along the center of the channel. The CCDs are 3 phase devices with a p-channel and 5-10 kΩ-cm substrate. The devices measured in our study were not backside processed, are 600 μm thick, and hence cannot be fully depleted. A detector bias of 50 V was used, resulting in a depletion region of about 300 μm.

The devices were irradiated at the Crocker Nuclear Laboratory (CNL) at the University of California at Davis. The Beam dosimetry is based on secondary emission monitor currents that are correlated to Faraday cup current measurements as described in [7]. The dosimetry uncertainty is less than 10%. The devices were irradiated with 63 MeV protons while unpowered at room temperature during irradiation. Three p-channel CCD devices were irradiated as part of our study, and they were designated LBL110, LBL112, and LBL115. LBL110 has no notch in the parallel registers and was exposed to 2.5 x 10^9 protons cm^{-2}. LBL112 and LBL115, with boron-implanted mini-channels in the parallel registers, were irradiated to 2.5 x 10^9 cm^{-2} and 5.0 x 10^9 cm^{-2}, respectively. During a second trip to CNL, LBL110 and LB L112 were both irradiated to an additional fluence of 5.44 x 10^{10} cm^{-2} protons for a total exposure of 5.7 x 10^{10} cm^{-2}.

2.1 CCD readout sequences

The p-channel CCD was read out in a manner that permitted both EPER and FPR measurements to be made during a single readout sequence. In addition, measurements were made with two different timing patterns to permit direct comparisons of the CTE results with those obtained by the Berkeley group on the same p-channel CCD, as well as with measurements performed by the NASA GSFC Detector Characterization Laboratory (DCL) group on the WFC3 E2V n-channel CCD (CCD43).

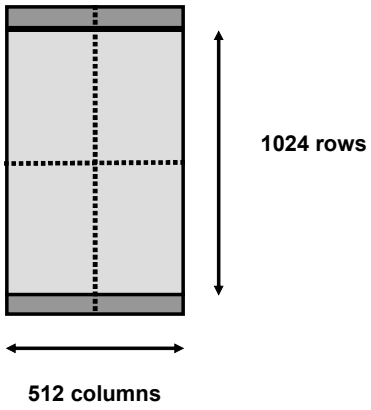

Figure 1: Split horizontal and vertical registers were used to obtain both EPER and FPR measurements.

To achieve the parallel EPER and FPR measurements from a single frame the CCD was exposed to flat field illumination and the entire device was readout using split modes in both the vertical (parallel) and horizontal (serial) registers as indicated in figure 1. The readout procedure described next is qualitatively pictured in figure 2. The lower 512x512 portion of the image was read out first through a lower amplifier. With clocks to the upper half of the array disabled, there were 620 rows shifted, including 512 of image (the lower half of the array) and 108 of overscan. This permitted an EPER measurement to be performed using the overscanned reads. Next, the lower 512 rows were read out to sweep any deferred charge from the lower half of the array and at the same time the upper 512 rows were clocked into the lower 512 rows. Another 512 clock cycles enabled an FPR measurement to be completed. This was followed by 156 rows of overscan to permit a second EPER measurement.

Wide Field 3 Timing To obtain the serial EPER and FPR measurements the serial register was read out through a single amplifier. First the half of the register (256 pixels) closest to the amplifier was read by clocking 370 pixels. This includes 6 prescan and 108 overscan clocks to permit the EPER measurement. Then the first 262 pixels were clocked out to clear the registers (including 6 prescan pixels), followed by the 256 pixels of image and 68 of overscan to permit EPER and FPR measurements.

To enable comparison with the E2V CCD43 data [5], the row times were matched to the WFC3 measurements by shifting an extra 575 pixels without reading to extend the row time to create an effective line readout time of (950 + 575) 30μs = 45.75 ms. (The readout time per pixel is 30 μs which includes the 8 μs clamp and 8 μs sample for an effective bandwidth of 62.5 kHz.) We refer to this as the WFC3 timing.

Berkeley Timing For comparisons to the data of Bebek, et al. [1] the readout sequence is similar except that for the serial readout sequence. First the half of the register (256 pixels) closest to the amplifier was read by clocking 280 pixels. This includes 6 prescan and 18 overscan clocks to permit the EPER measurement. Then the first 262 pixels were clocked out to clear the registers, followed by the 256 pixels of image and 10 of overscan to permit EPER and FPR measurements. In the Berkeley case, it was not necessary to shift any extra pixels to match the effective line readout time of 810 x 30μs = 24.3 ms.

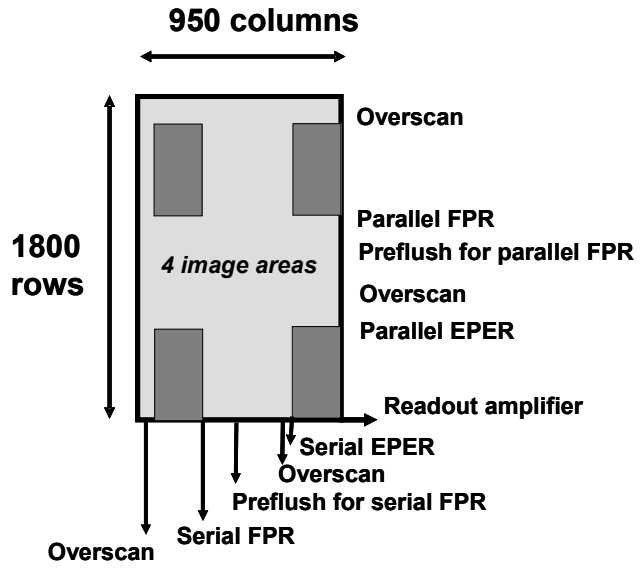

Figure 2: Pictorial showing the acquisition of the EPER and FPR data during a single readout sequence for the WFC3 timing pattern. Dark shaded areas represent the physical image area of 1024 rows by 512 columns, and light regions indicate the overscan and preflush timing sequences used to read out the split serial and split parallel areas.

3. THE EPER, FPR, AND ^{55}FE CTE RESULTS

The ^{55}Fe technique was used to obtain an absolute measurement of the charge transfer inefficiency, or CTI (CTI = 1-CTE), in a manner directly comparable to both the LBNL p-channel CCD [1] as well as the E2V n-channel CCD [5] results. The CTI at -83°C was characterized using WFC3 timing as a function of x-ray density as shown in figure 3 after exposure to 2.5 x 10^9 cm^{-2} and 5.0 x 10^9 cm^{-2} 63 MeV protons. The abscissa gives the x-ray density in terms of the delta time (or time between events). This may be converted to x-ray density by consideration of the 45 ms time to read out a 1024 pixel row. For example, a delta time of 2.6 s corresponds to an average x-ray density of one event per 60 pixels. Clearly, the CTI is very dependent on the x-ray density, which must be specified when comparing CTI results between measurements. Also apparent is the significant improvement in CTE afforded by the notched CCD as opposed to the CCD with no notch after 2.5 x 10^9 cm^{-2}, especially for the case of very sparse x-ray events.

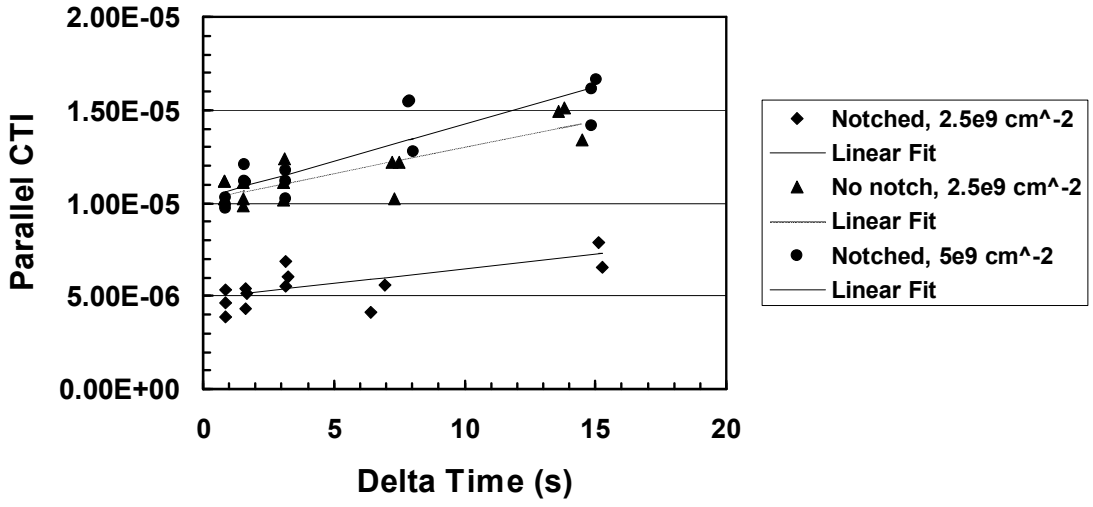

Figure 3: ^{55}Fe results as a function of x-ray density for LBNL p-channel CCDs acquired at -83°C using WFC3 timing.

The EPER technique was used to determine CTI of a notched p-channel CCD as a function of signal size in the case of WFC3 timing. Figure 4 shows the results for a notched p-channel CCD at -140°C after 5 x 10^9 cm^{-2} 63 MeV protons. The EPER measurement uses a flat field illumination, and estimates the amount of deferred charge found in either the parallel or serial extended pixel region by over clocking the charge [e.g. 5]. Typically a number of lines are averaged together to improve the signal-to-noise ratio in the extended pixel region. Figure 4 also compares the EPER results with the ^{55}Fe x-ray measurement, and we note that the two yield the same answer when the x-ray density corresponds to a delta time of 20 s. As discussed in [5], these are two fundamentally different methods of characterizing CTE, and there is no *a priori* cause for the methods to yield the same result. No evidence of the notch overflowing is apparent out to a signal size of 20,000 carriers.

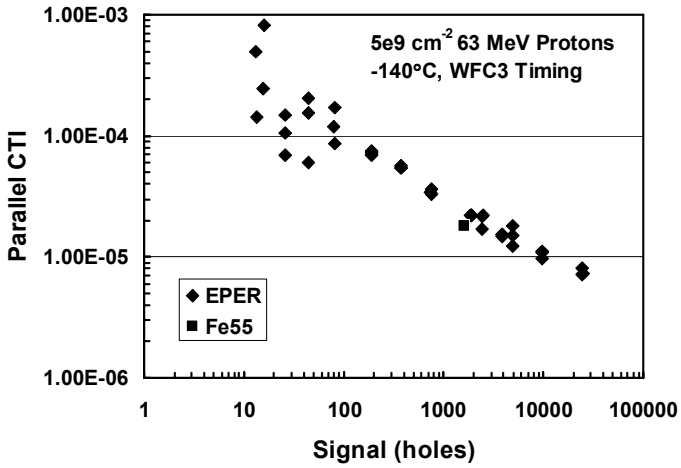

Figure 4: The parallel CTI is shown as a function of signal level at -140°C for a notched p-channel CCD irradiated with 5 x 10^9 cm^{-2} 63 MeV protons. The ^{55}Fe measurement (delta time = 20s) is comparable to the EPER results.

The ^{55}Fe CTE is plotted as a function of temperature for an average x-ray density of 1 hit per 60 pixels in figure 5. The temperature dependence is qualitatively consistent with the results of Bebek et al. [2], which were measured with an x-ray density of about 1 hit per 70 pixels after exposure to 12 MeV protons. As seen in the figure the absolute values of the CTI and the temperature dependencies are generally comparable for both the WFC3 and LBNL timing. Attempts were made to study the p-channel CCD CTE at warmer temperatures, e.g. up to -30°C or warmer, however, the devices used in this study were not thinned, and this resulted in high dark currents. The associated "fat zero" effects of the elevated dark currents made warm CTE studies impossible.

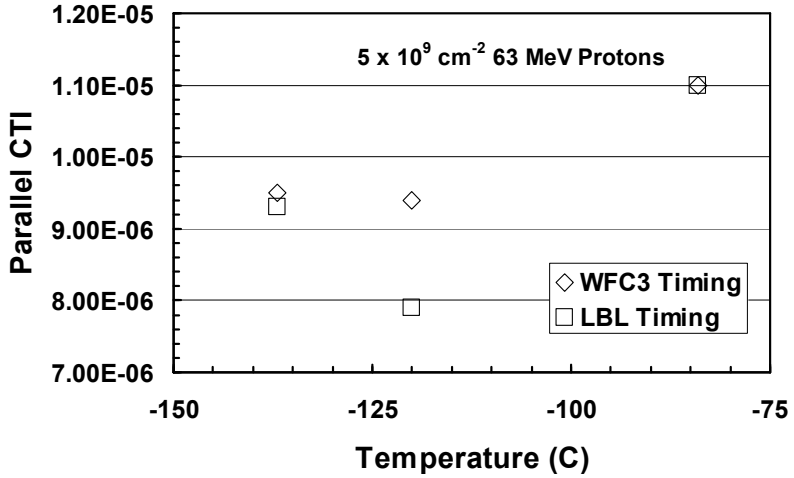

Figure 5: The temperature dependence of the parallel CTI is shown as measured by ^{55}Fe after irradiation of LBL115 to 5 x 10^9 cm^{-2} 63 MeV protons. For n-channel CCDs, the expected trend would be towards significantly higher CTI at lower temperatures due the trapping effects of the oxygen-vacancy complex.

The EPER results for p-channel CCDs with a 3 μm mini-channel and without a mini-channel, are compared in figure 6. We observe roughly a factor of two improvement in CTI for the device with the mini-channel, in agreement with the results of Bebek et al. [1]. Note that once the signal level exceeds the notch capacity, the charge spills out of the mini-channel and the CTE is expected to revert to values it would have without the notch. Interestingly, a similar improvement was observed between the notched versus un-notched WFC3 E2V n-channel CCDs.

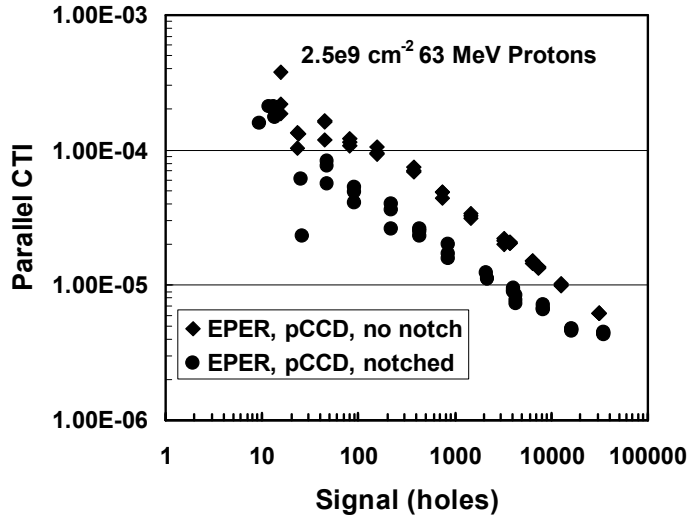

Figure 6: Comparison of p-channel CCDs with and without a notch after exposure to 2.5e9 cm^{-2} 63 MeV protons.

As shown in figure 7, at -84°C the CTI degradation of the p-channel CCD (with or without a notch) is almost an order of magnitude less severe as compared to the n-channel CCD43 (with a notch) and CCD44 (without a notch), respectively. All measurements were performed using WFC3 timing. It is worth noting that the p-channel CCD versus n-channel CCD improvement factor would be expected to vary with temperature, and this comparison is made at a temperature that is optimized for the n-channel CCD. Greater than 10x improvement would be expected at other temperatures.

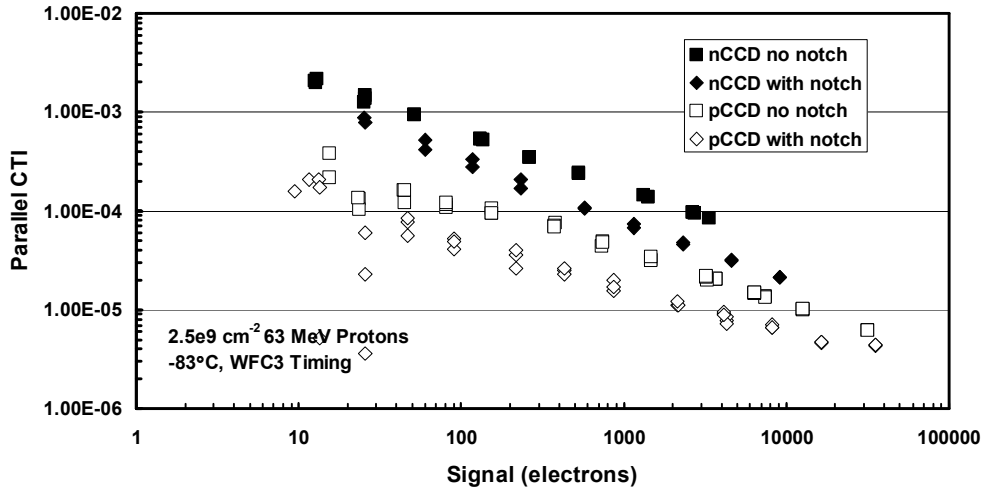

Figure 7: Comparison of n-channel CCDs and p-channel CCDs both with and without notches after exposure to 2.5e9 cm^{-2} 63 MeV protons. The CTI improvement relative to the n-channel CCD depends some on the signal level but is a factor of 5 to an order of magnitude.

In figure 8, the p-channel CCD ^{55}Fe x-ray CTE values at two proton fluences are compared to those obtained for the WFC3 n-channel CCD [6]. The p-channel CCD CTE is seen to be significantly less degraded as a function of fluence than the n-channel CCD. The present n versus p-channel CCD comparison is made more straightforward than was possible in [1] because we are comparing identical timing and measurement conditions, as well as more similar 63 MeV proton exposure levels. The improvement afforded by the notch technology is once again illustrated in figure 9 which shows the p-channel CCD CTE as a function of proton fluence. One can also note that the CTE degradation is linear with proton fluence. This figure also shows a direct comparison with the irradiations in Bebek et al. [2] performed using very similar measurement conditions. Note that since the Bebek proton exposures were at 12 MeV (versus our 63 MeV) we had to approximate the effective damage that would have been produced at 63 MeV. The equivalent 63 MeV fluence was calculated by normalizing the displacement damage dose using the nonionizing energy loss rate (NIEL) function for proton damage in Si [8]. The 12 MeV protons are more damaging per unit fluence by a factor of about 2.

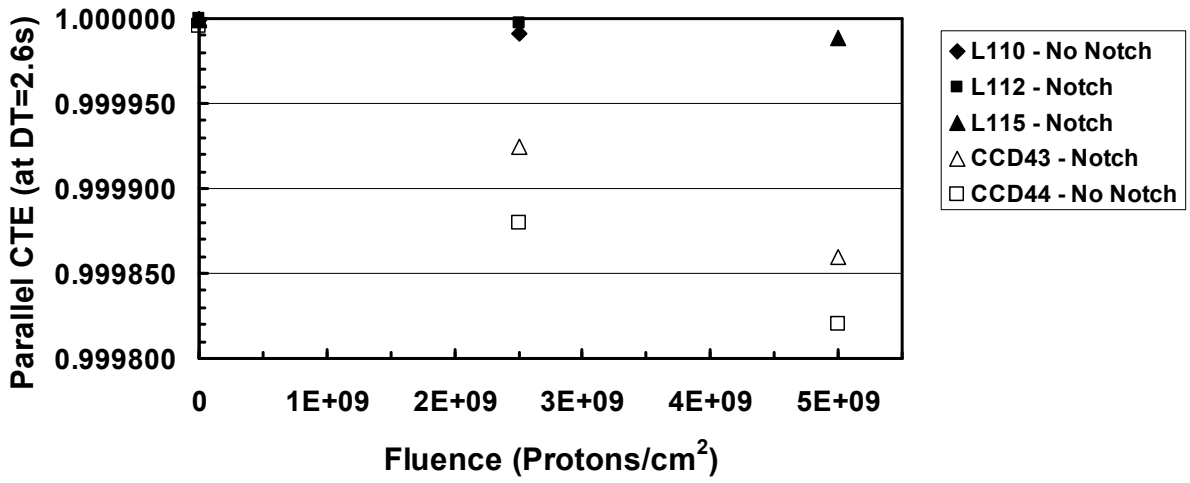

Figure 8: The CTI at -84°C is shown for the current p-channel CCD and compared to the WFC3 n-channel CCD results of Waczynski et al. [6] as a function of 63 MeV proton fluence. The x-ray densities are comparable (1in 60 pixels for the WFC3 n-channel CCD and our p-channel CCD results). The WFC3 timing was used for all measurements.

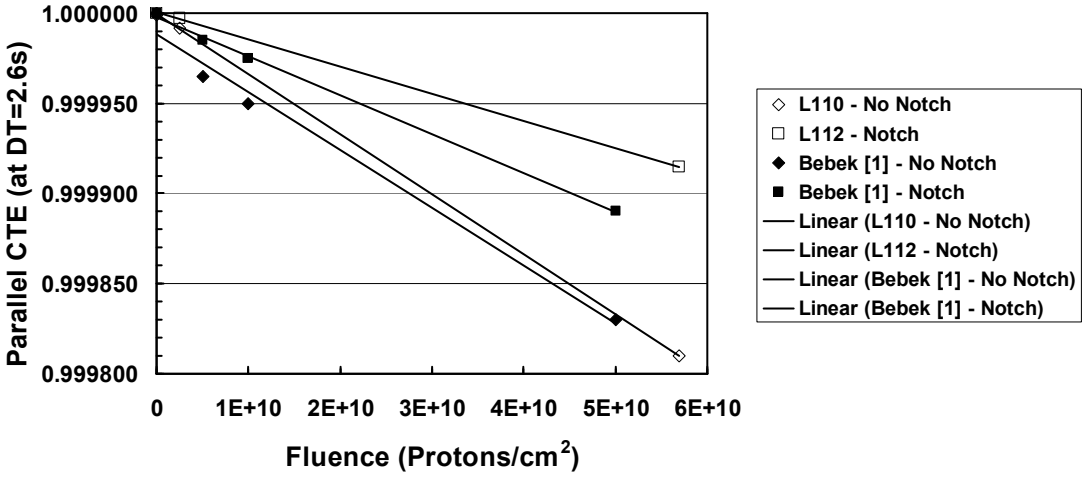

Figure 9: The CTI at -84°C is shown for the current p-channel CCD and compared to the p-channel CCD results of Bebek et al. [1] as a function of equivalent 63 MeV proton fluence. The x-ray densities are comparable (1in 60 pixels for the WFC3 n-channel CCD and our p-channel CCD results, and 1 in 70 pixels for Bebek et al.). The Berkeley timing was used for these measurements.

The FPR technique is similar to EPER, but measures the charge missing from the leading edge of a flat field image [5 and references therein]. At lower proton fluences, the FPR measurements were difficult to extract as a result of the shot noise on the optical flat field signal. The data of figure 10 show comparisons of EPER and FPR CTI results at higher proton fluences for -137°C, and the results were very similar at -83°C, though the data are not shown here.

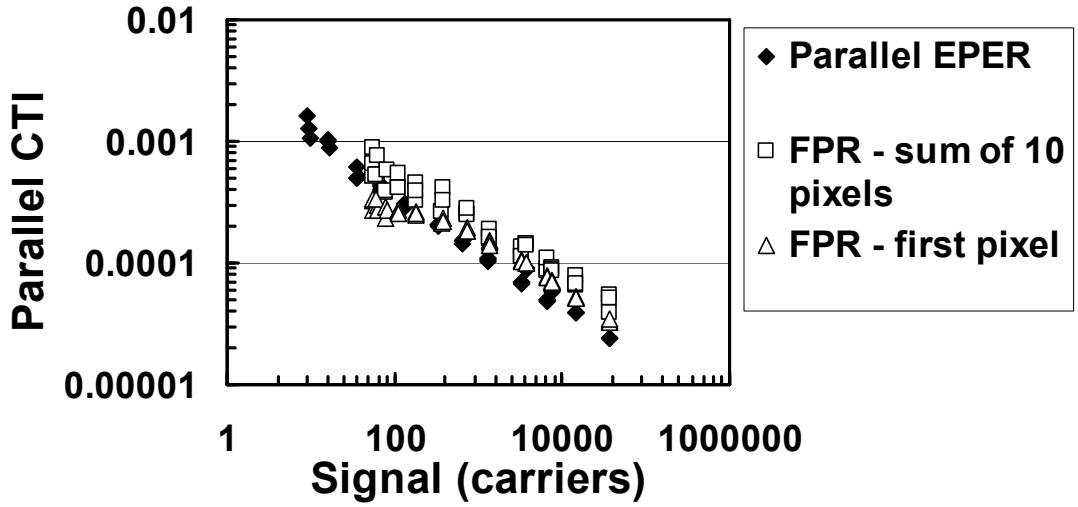

Figure 10: Parallel CTI results using both EPER and FPR as a function of signal at -137°C after exposure to 5.69 x 10^{10} cm^{-2} 63 MeV protons. The FPR obtained by integrating the charge loss in the leading edge over 10 pixels yields slightly higher CTI values than the other two techniques.

4. THE PROTON-INDUCED DARK CURRENT BEHAVIOR

The dark current was measured as follows. For each measurement condition, a series of long dark frames (e.g. 1 hour) was acquired. A short (1 second) "super bias frame" was taken and subtracted from the long dark frames to remove distortion in the baseline due to the readout. Cosmic ray rejection was difficult because of instability in the dark frames. To combat this multiple long darks were taken and the frames selected for analysis were those acquired after the dark current had leveled off. If a pixel exceeds the mean + 4 sigma, but goes low for one of the files then it is rejected as a cosmic ray. In addition, the pre-irradiation dark current histogram is used to make a map of "bad pixels" (defined as a pixel with a dark current exceeding the mean plus 4 sigma in more than 1 frame) that are subtracted from the post-irradiation histograms. The radiation-induced high dark current pixels are evident in figure 11 (b) and (c) which compares the pre- and post-irradiation dark current histograms at exposure levels of 2.5 x 10^{9} protons cm^{-2} and 5.69 x 10^{10} cm^{-2}, respectively. The p-channel CCD technology is evidently not hardened as compared to n-channel CCDs with respect to the formation of hot pixels based on these data acquired at -83°C. This differs from the results reported by Bebek [1], however this is not inconsistent since those data were measured at -140°C and hot pixels may have been effectively suppressed by cooling. Such hot pixels reduce pixel operability for science and star-tracking applications. As a result of the very different noise levels and peak shapes, it was not possible to perform a quantitative comparison of the percent hot pixels per unit fluence between the n- and p-channel CCDs. Note that the peak dark current levels increase linearly with fluence as expected.

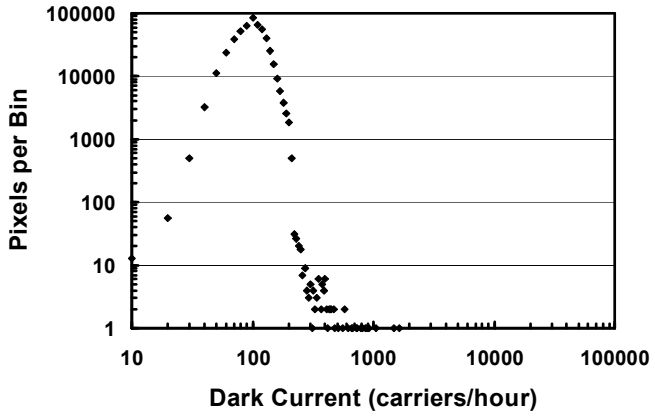

(a)

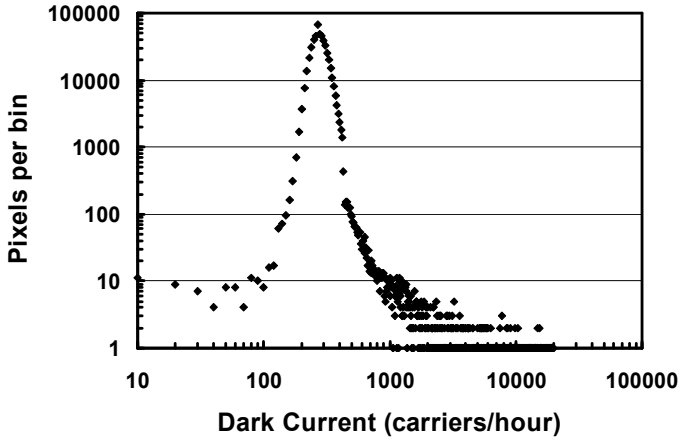

(b)

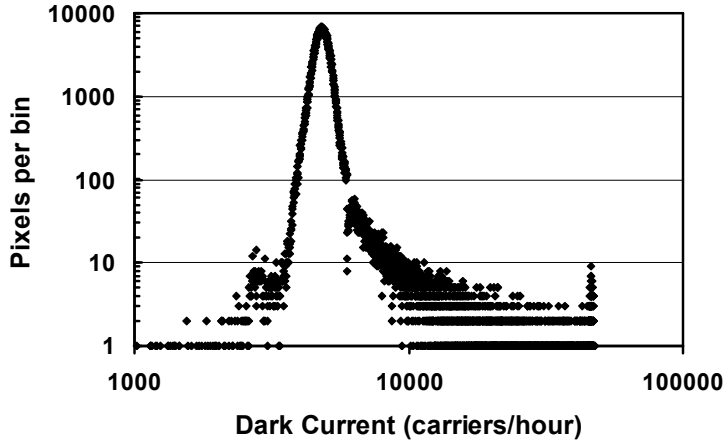

(c)

Figure 11: (a) Pre-irradiation dark current histogram at -83°C, (b) dark current histogram showing hot pixels at -83°C for a device irradiated with 2.5×10^{9} cm^{-2} 63 MeV protons, and (c) dark current histogram showing hot pixels at -83°C for a device irradiated with 5.69×10^{10} cm^{-2} 63 MeV protons .

5. SUMMARY

The proton-induced charge transfer efficiency (CTE) behavior for the Lawrence Berkeley National Laboratory (LBNL) p-channel CCD (being developed for the SuperNova Acceleration Probe (SNAP)) and Hubble Space Telescope (HST) Wide Field Camera 3 (WFC3) n-channel CCDs are compared using ^{55}Fe and EPER measurements. Berkeley p-channel CCDs fabricated at Dalsa both with and without mini-channels in the parallel registers are compared to the E2V, Inc. CCD43 (a notched, multi-phase pinned (MPP) device) and the E2V CCD44 (an un-notched, non-MPP device), using the same readout timing and measured over the same range of temperatures. At -83°C, where n-channel CCDs are optimized for minimal CTE degradation, the CTE performance of the p-channel CCD is about an order of magnitude better than the E2V n-channel CCD after a 63 MeV fluence of 2.5 x 10^9 cm^{-2}. In addition, the notched devices of both types (n- and p-channel CCD) exhibited about a factor of two improvement in the CTE as compared to their un-notched counterparts. In contrast, the hot pixels remain an issue for p-channel devices operated at warmer temperatures, just as they are for n-channel CCDs. Finally, our CTE measurements compared reasonably well with previous CTE measurements at 12 MeV by Bebek et al. [1]

ACKNOWLEDGEMENTS

We would like to acknowledge the support of the NASA Electronics and Packaging Program (NEPP) and the Defense Threat Reduction Agency (DTRA). We also appreciate the technical support from Chris Bebek and Armin Karcher at the Lawrence Berkeley National Laboratory.

REFERENCES

1. C. Bebek, D. Groom, S. Holland, A. Karcher, W. Kolbe, J. Lee, M. Levi, N. Palaio, B. Turko, M. Uslenghi, M. Wagner, and G. Wang, "Proton Radiation Damage in P-Channel CCDs Fabricated on High-Resistivity Silicon," IEEE Trans. Nucl. Sci., Vol. 49, No. 3, 2002, pp. 1221-1225.

2. J.P. Spratt, B.C. Passenheim, and R.E. Leadon, "The effects of nuclear radiation on P-channel CCD imagers," in Proc. 1997 Radiation Effects Data Workshop (NSREC), Snowmass, CO 1997, pp. 116-121.

3. C.J. Bebek, D.E. Groom, S.E. Holland, A. Karcher, W.F. Kolbe, J. Lee, M.E. Levi, N.P. Palaio, B.T. Turko, M.C. Uslenghi, M.T. Wagner, and G. Wang, "Proton radiation damage in high-resistivity n-type silicon CCDs, Proc. SPIE, Vol. 4669, 2002, pp. 161-171.

4. G.R. Hopkinson, "Proton damage effects on P-channel CCDs," IEEE Trans. Nucl. Sci., Vol. 46, No. 6, 1999, pp. 1790-1796.

5. A. Waczynski, E.J. Polidan, P.W. Marshall, R.A. Reed, S.D. Johnson, R.J. Hill, G.S. Delo, E.J. Wassell, and E.S. Cheng, "A Comparison of Charge Transfer Efficiency Measurement Techniques on Proton-Damaged n-Channel CCDs for the Hubble Space Telescope Wide-Field Camera 3," IEEE Trans. Nucl. Sci., Vol. 48, No. 6, 2001, pp. 1807-1814.

6. E.J. Polidan, A. Waczynski, P. Marshall, S.D. Johnson, C. Marshall, R. Reed, R.A. Kimble, G. Delo, G. Schlossberg, A.M. Russell, T. Beck, Y. Wen, J. Yagelowich, R.J. Hill, and E. Wassell, "Hot pixel behavior in WFC3 CCD detectors irradiated under operational conditions, Proc. SPIE 2003, Vol. 5167, 2004, pp. 258-269.

7. C. M. Castenada, "Crocker Nuclear Laboratory (CNL) radiation effects measurement and test facility," in Proc. 2001 Radiation Effects Data Workshop (NSREC), Vancouver, British Columbia, 2001, pp. 77-81.

8. C.J. Dale, L. Chen, P.J. McNulty, P.W. Marshall, and E.A Burke, "A Comparison of Monte Carlo and Analytic Treatments of Displacement Damage in Microvolumes," IEEE Trans. Nucl. Sci., Vol. 41, No. 6, pp. 1974-1983, 1994.